Brain Research 1818 (2023) 148517

Contents lists available at ScienceDirect

Brain Research

journal homepage: www.elsevier.com/locate/brainres

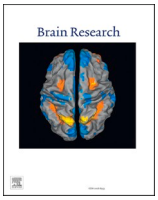

Galectin-1 as a marker for microglia activation in the aging brain

Tamas Kiss [a,b,i,1], Yaqub Mir [c,d,e,1], Gergely Stefancsik [c], Gantulga Ganbat [c], Aruzhan Askarova [c], Eva Monostori [f], Karolina Dulka [c], Gabor J. Szebeni [g,h], Ádám Nyúl-Tóth [b,i,j,k], Anna Csiszár [b,c,i,j,l], Adam Legradi [c,*]

[a] Pediatric Center, Semmelweis University, Budapest, Hungary
[b] Vascular Cognitive Impairment, Neurodegeneration and Healthy Brain Aging Program, Department of Neurosurgery, University of Oklahoma Health Sciences Center, Oklahoma City, OK, USA
[c] Department of Cell Biology and Molecular Medicine, University of Szeged, Szeged, Hungary
[d] Department of Computational Sciences, Wigner Research Centre for Physics, Budapest, Hungary
[e] Department of Anatomy, Histology and Embryology, Semmelweis University, Budapest, Hungary
[f] Lymphocyte Signal Transduction Laboratory, Institute of Genetics, Biological Research Centre, Szeged, Hungary
[g] Laboratory of Functional Genomics, Biological Research Centre, ELKH, Szeged, Hungary
[h] Department of Physiology, Anatomy and Neuroscience, Faculty of Science and Informatics, University of Szeged, Szeged, Hungary
[i] Oklahoma Center for Geroscience and Healthy Brain Aging, University of Oklahoma Health Sciences Center, Oklahoma City, OK, USA
[j] International Training Program in Geroscience, Doctoral School of Basic and Translational Medicine/Departments of Public Health and Translational Medicine, Semmelweis University, Budapest, Hungary
[k] Institute of Biophysics, Biological Research Centre, ELKH, Szeged, Hungary
[l] The Peggy and Charles Stephenson Cancer Center, University of Oklahoma Health Sciences Center, Oklahoma City, OK, USA

ARTICLE INFO

Keywords:
Microglia
Aging
Galectin-1
Neuroinflammation

ABSTRACT

Microglia cells, the immune cells residing in the brain, express immune regulatory molecules that have a central role in the manifestation of age-related brain characteristics. Our hypothesis suggests that galectin-1, an anti-inflammatory member of the beta-galactoside-binding lectin family, regulates microglia and neuroinflammation in the aging brain. Through our *in-silico* analysis, we discovered a subcluster of microglia in the aged mouse brain that exhibited increased expression of galectin-1 mRNA. In our Western blotting experiments, we observed a decrease in galectin-1 protein content in our rat primary cortical cultures over time. Additionally, we found that the presence of lipopolysaccharide, an immune activator, significantly increased the expression of galectin-1 protein in microglial cells. Utilizing flow cytometry, we determined that a portion of the galectin-1 protein was localized on the surface of the microglial cells. As cultivation time increased, we observed a decrease in the expression of activation-coupled molecules in microglial cells, indicating cellular exhaustion. In our mixed rat primary cortical cell cultures, we noted a transition of amoeboid microglial cells labeled with OX42(CD11b/c) to a ramified, branched phenotype during extended cultivation, accompanied by a complete disappearance of galectin-1 expression. By analyzing the transcriptome of a distinct microglial subpopulation in an animal model of aging, we established a correlation between chronological aging and galectin-1 expression. Furthermore, our in vitro study demonstrated that galectin-1 expression is associated with the functional activation state of microglial cells exhibiting specific amoeboid morphological characteristics. Based on our findings, we identify galectin-1 as a marker for microglia activation in the context of aging.

Abbreviations: ANOVA, Analysis of variance; CNS, Central nervous system; CD11b (Itgam), Integrin alpha M; CD14, Myeloid specific leucine rich glycoprotein; CD16(Fcgr3), Fc gamma receptor III; CD40, TNF receptor subfamily member 5; CD163, Scavanger receptor; CD206(Mrc1), Mannose receptor; DAP12, DNAX activation protein of 12kDa; DMEM, Dulbecco's modified Eagle's medium; FBS, Fetal bovine serum; Gal-1, Galectin-1; Iba1, Ionized calcium binding adapter molecule 1; MCSF, Macrophage colony stimulating factor; PBS, Phosphate-buffered saline; RT, Room temperature; RT1A, MHC1 molecule; SEM, Standard error of the mean; SiglecH, Sialic acid receptor; TBS, Tris-buffered saline; TI, Transformation index; TNF, Tumor necrosis factor; UMAP, Uniform manifold approximation and projection.

* Corresponding author at: Department of Cell Biology and Molecular Medicine, University of Szeged, Somogyi utca 4, Szeged H-6720, Hungary.
E-mail addresses: kiss.tamas1@med.semmelweis-univ.hu (T. Kiss), dulka.karolina@med.u-szeged.hu (K. Dulka), szebeni.gabor@brc.hu (G.J. Szebeni), adam-nyultoth@ouhsc.edu (Á. Nyúl-Tóth), anna-csiszar@ouhsc.edu (A. Csiszár), legradam@bio.u-szeged.hu (A. Legradi).
[1] These authors are equally contributed to this work.

https://doi.org/10.1016/j.brainres.2023.148517
Received 19 April 2023; Received in revised form 21 July 2023; Accepted 2 August 2023
Available online 7 August 2023

1. Introduction

Aging is a multifaceted and ever-evolving biological phenomenon, characterized by the ongoing reconfiguration of cellular brain functionality. Among the defining features of aging, there exists a subclinical, persistent, low-intensity sterile inflammation commonly referred to as "inflammaging" (Frasca and Blomberg, 2016, Williamson et al., 2011, López-Otín et al., 2013).

Microglial cells, belonging to the monocyte/macrophage lineage (Kreutzberg, 1996; Prinz et al., 2011), originate from primitive myeloid yolk sac-localized progenitors and represent a distinct population within the mononuclear phagocyte system (Hoeffel et al., 2015; Ginhoux et al., 2010). Present throughout the central nervous system (CNS), microglia exist as a continuum of various morphological phenotypes, ranging from amoeboid to extensively ramified forms. Activation of microglia leads to a transformation from amoeboid to extensively ramified types, accompanied by morphological changes. Additionally, functional alterations such as microglial proliferation, homing and adhesion to damaged cells, and robust phagocytic activity can be observed (Town et al., 2005). The amoeboid appearance and phagocytic nature of microglia coincide with their ability for antigen presentation (Szabo and Gulya, 2013) as well as their involvement in cytotoxic and inflammation-related signaling (Kata et al., 2016; Kata et al., 2017). Importantly, the presence of chronic, low-grade neuroinflammation involving activated/primed microglial cells has been linked to age-related CNS disorders, including Alzheimer's disease (Heneka et al., 2015; Leng and Edison, 2021; Williamson et al., 2011).

Galectin-1 (Gal-1), a member of a highly conserved lectin family, exhibits binding affinity towards the common disaccharide Galβ1-4GlcNAc present on N- and O-glycans, thereby modifying cell surface glycoconjugates (Hirabayashi and Kasai, 1993). Gal-1 serves diverse functions, exerting intracellular effects such as mRNA splicing (Liu et al., 2002; Park et al., 2001) as well as extracellular roles in cell growth regulation, apoptosis induction, immunomodulation, cell transformation, and cancer development (Camby et al., 2006). The anti-inflammatory and immunomodulatory properties of Gal-1 have been previously demonstrated, with activated macrophages (Rabinovich et al., 1996), antigen-stimulated T cells (Blaser et al., 1998), activated B cells (Zuñiga et al., 2001), and alloreactive T cells (Rabinovich et al., 2002) shown to secrete high levels of Gal-1. It is hypothesized that Gal-1 plays a role in eliminating effector T cells once the immune response is complete. Moreover, our previous studies have revealed the immunoregulatory activity of Gal-1, exemplified by tumor-derived Gal-1-induced apoptosis of activated T cells (Ion et al., 2006; Kovács-Sólyom et al., 2010). The Gal-1 protein associated with mesenchymal stem cells appears to act as a key regulator of tumor growth (Szebeni et al., 2012). Within the central nervous system (CNS), Gal-1 governs the proliferation of adult neural progenitor cells (Sakaguchi et al., 2006), regulates neurogenesis, and promotes functional recovery following stroke (Ishibashi et al., 2007). Furthermore, the expression of Gal-1 correlates with the regenerative potential of spinal motoneurons after spinal cord injury (McGraw et al., 2004).

Despite the well-established role of Gal-1 in inflammatory processes, its presence and function in microglial cells remain unknown. Our hypothesis posits that Gal-1 serves as a key regulator of neuroinflammation associated with microglia in the aging brain.

2. Experimental procedures

2.1. Animals

All animal experiments were carried out in strict compliance with the European Council Directive (86/609/EEC) and EC regulations (O.J. of EC No. L 358/1, 18/12/1986) regarding the care and use of laboratory animals for experimental procedures and followed the relevant Hungarian legislation's requirements. The Institutional Animal Welfare Committee of the University of Szeged (II./1131/2018) approved the experimental protocols.

2.2. In silico single-cell analysis

The single-cell RNA sequencing database of the aged mouse brain was acquired from the Single-Cell Portal website of the Broad Institute [https://singlecell.broadinstitute.org/single_cell] in the form of a normalized count matrix. Ximerakis and his colleges isolated brain cells from 2 to 3 and 21–22-month-old, male C57BL/6J mice and loaded them onto a 10× Genomics chromium single-cell 3′ chip. The cDNA library preparation was conducted using the 10× Genomics chromium single-cell 3′ library with a Gel Bead kit v2 and an i7 Multiplex kit, and the libraries were sequenced on an Illumina NextSeq 500 instrument. Further experimental details are included in the original publication (Ximerakis et al., 2019). Cell-type-specific clustering from the original study was preserved and utilized to further subdivide the original data set. The gene expression profiles of microglia subsets were processed by the Seurat workflow V4 in R environment (Stuart et al., 2019). After an initial quality control, 3,885 microglia cells (1,651 young, 2,234 aged) were analyzed, scaling and linear dimensional reduction (principal component analysis) were performed using the default parameters. The number of relevant principal components for further downstream analysis was identified by a resampling test known as the JackStraw procedure (Chung and Storey, 2015). 2D embedding was performed by the uniform manifold approximation and projection (UMAP) method (Becht et al., 2019) using the top 20 principal components. To cluster our cells, after creating a graph structure, we used the Louvain algorithm as a modularity optimization technique. The resolution factor was set to 0.3. All the previous steps were performed on the microglia cluster without separating the cells from the aged and young animals. Cells expressing *Gal-1* mRNA were considered Gal-1-positive and were counted, regardless of the expression levels. A chi-square test of independence was performed to examine the relationship between the subcluster and Gal-1 positivity. Wilcoxon Rank Sum test was used to identify genes differentially expressed in the individual sub-clusters with the adjusted p-value threshold<0.05. The overrepresentation analysis of Gene Ontology terms on the differentially expressed genes was performed using g:Profiler (31066453). Terms including more than 1000 or<6 genes were excluded to improve interpretability of the result.

2.3. Preparation of mixed primary neuronal and microglial enriched secondary cell cultures

To study the activation state of the Gal-1-expressing microglial cells, an in vitro model system was used. Mixed primary cortical cell cultures from newborn, wild-type SPRD rats were established using the methods described previously (Szabo and Gulya, 2013). In brief, newborn rats were surgically decapitated and the frontal lobe of the cerebral cortex was removed. The harvested tissue was minced with scissors, then incubated for 10 min at 37 °C in 9 mL of Dulbecco's modified Eagle's medium (DMEM; Invitrogen, Carlsbad, CA, USA) containing 1 g/L D-glucose, 110 mg/L Na-pyruvate, 4 mM L-glutamine, 3.7 g/L $NaHCO_3$, 10,000 U/mL penicillin G, 10 mg/mL streptomycin sulfate, and 25 μg/mL amphotericin B, supplemented with 0.25% trypsin (Invitrogen), and then centrifuged at 1000 × *g* at room temperature (RT) for 10 min. The pelleted cells were resuspended and washed twice in 5 mL of DMEM containing 10% heat-inactivated fetal bovine serum (FBS; Invitrogen). Following the final washing step, cells were seeded either onto poly-L-lysine-coated coverslips (15 × 15 mm; 2×10^5 cells/coverslip) or in a poly-L-lysine-coated T75 flask (1×10^7 cells/flask) (Corning, New York, NY, USA) and cultured at 37 °C in a humidified atmosphere supplemented with 5% CO_2. Primary mixed neuronal cultures were maintained for 7 (DIV7), 14 (DIV14), or 21 (DIV21) days. The culture media was changed every 3 days.

A microglia-enriched cell culture was prepared from the mixed

primary cultures maintained in the poly-L-lysine-coated culture flasks (1×10^7 cells/flask). To collect the microglial cells from the mixed neuronal cultures on DIV7 and DIV14, the cultures were subcloned by shaking at 150 rpm in an orbital platform shaker at 37 °C for 30 min. Alternatively, primary mixed neuronal cultures were shaken at 37 °C at 150 rpm for 3 h in a platform shaker to collect enough microglial cells for the anti-Gal-1 Western blot experiments and for lipopolysaccharide (LPS; Sigma, St. Louis, MO, USA) stimulation.

Microglia from the supernatant were collected by centrifugation at 3000 × *g* at RT for 8 min and resuspended in 2 mL DMEM/10% FBS. Cells were seeded at a density of 4×10^5 cells/petri dish for Western blotting analyses and cultured in DMEM/10% FBS in a humidified atmosphere supplemented with 5% CO_2 at 37 °C for 5 days. After 5 days of culturing the collected microglia, cultures were treated with 20 ng/mL LPS for 24 h.

2.4. Western blotting analyses

Cells from DIV7, DIV14, and DIV21 primary mixed neuronal cell culture and cells from the bacterial LPS-treated (20 ng/mL) microglia-enriched cultures were collected and homogenized in 50 mM Tris-HCl (pH 7.5) (Sigma) containing 150 mM NaCl, 0.1% Nonidet P40 (Sigma), 0.1% cholic acid (Sigma), 2 μg/mL leupeptin (Sigma), 1 μg/mL pepstatin (Sigma), 2 mM phenylmethylsulfonylfluoride (Sigma), and 2 mM EDTA (Sigma), and then centrifuged at 10,000 × *g* for 10 min. The pellet was discarded and the protein concentration of the supernatant was measured (Lowry et al., 1951). For the Western blotting analyses, 5 μg of protein was separated on a sodium dodecyl sulfate/polyacrylamide gel (4% stacking gel, 12% resolving gel), transferred onto a Hybond-ECL nitrocellulose membrane (Amersham Biosciences, Little Chalfont, Buckinghamshire, England), blocked for 1 h with 5% nonfat dry milk in Tris-buffered saline (TBS) containing 0.1% Tween 20, and incubated overnight either with rabbit anti-Gal-1 polyclonal antibody (1:500 final dilution; gifted by the Monostori's lab; Vas et al., 2005) or mouse anti-GAPDH monoclonal antibody (clone GAPDH-71.1; 1:20,000; Sigma). The membranes were rinsed five times in 0.1% TBS-Tween 20 and incubated for 1 h with peroxidase-conjugated goat anti-rabbit IgG (1:2000 final dilution; Invitrogen) for Gal-1 detection or with peroxidase-conjugated rabbit anti-mouse IgG (1:2000 dilution; Sigma) for GAPDH detection. The enhanced chemiluminescence method (ECL Plus Western blotting detection reagents; Amersham Biosciences) was used to reveal immunoreactive bands according to the manufacturer's protocol. For Western blot image analysis, gray-scale digital images were acquired by scanning autoradiographic films. Bands were analyzed through the use of ImageJ software (version 1.38; developed by W. Rasband at the U.S. National Institutes of Health, and available from the Internet at http://rsb.info.nih.gov/ij). The immunoreactive densities of equally loaded lanes were quantified.

2.5. Fluorescence immunocytochemistry

Primary mixed neuronal cell cultures (DIV7, DIV14, DIV21) were fixed on coverslips with 4% formaldehyde for 5 min and rinsed three times for 5 min each with 0.05 M phosphate-buffered saline (PBS). After permeabilization and blocking of the nonspecific sites in PBS solution containing 5% normal goat serum (Sigma), 1% heat-inactivated bovine serum albumin (Sigma), and 0.05% Triton X-100 for 30 min at 37 °C, the cells were incubated overnight in a humidified chamber at 4 °C with mouse anti-CD11b/c (OX42) monoclonal antibody (1:50 final dilution; Invitrogen) and rabbit polyclonal anti-Gal-1 antibody (1:100 final dilution; Monostori's lab [Vas et al., 2005]). The cultured cells were washed in PBS four times for 10 min each at RT and incubated with Alexa Fluor 568-conjugated goat anti-rabbit antibody (1:1000 final dilution; Invitrogen) and Alexa Fluor 488-conjugated goat anti-mouse antibody (1:1000 final dilution; Invitrogen) in the dark for 3 h at RT. Cells were washed in PBS four times for 10 min each time at RT, then the coverslips were rinsed in distilled water for 5 min, air-dried, and mounted on microscope slides in ProLong Gold Antifade Mountant with DAPI mounting medium (InVitrogen,Waltham Massachutes, USA).

2.6. Determination of exhausted microglia cell burden by flow cytometric analysis

For further analysis, starter culture and isolated microglia cells in different time points were fixed in 1 % PFA in room temperature. After samples have been collected from all time points fixed cells have been washed in PBS then centrifuged (300×g, 10 min) and resuspended in MACS buffer (Miltenyi Biotech). To analyze microglia activation and subsequent exhaustion, we used quantitative fluorescent flow cytometry. Cells were labelled with an antibody directed against the microglia activation markers. 130 μl sorted cells were plated on a 96-well plate and incubated with 10 μl of 1% BSA (Sigma) in 2.8% Triton X-100 surfactant (EMD Chemicals Inc., TX1568-1) for 15 min. Then diluted antibody mix in MACS buffer was added into the wells up to 150 μl to achieve final concentration (Table 1.) and incubated another 30 min on a horizontal shaker (100 RPM, room temperature). The measurement was assessed on a Guava® EasyCyte™ BGR HT Flow Cytometer (Luminex) based on the manufacturer's recommendations. Data were analyzed using FCS Express software (De Novo Software). The ratio of stained and unstained cells was determined as a percentage of total cells. Cell debris was gated out during measurement and also in flow cytometry data analysis (for gating strategy see Fig. 7).

2.7. Flow cytometry for cell surface bound Gal-1 detection

Microglia cells derived from DIV7, DIV14, or DIV21 primary mixed neuronal cell cultures were isolated by shaking at 150 × *g* in a platform shaker for 30 min. Cells were labeled with polyclonal anti-Gal-1 antibody (produced in Eva Monostori's laboratory, Vas et al., 2005) and incubated at 4 °C for 1 h. Cell surface-bound antibodies were labeled with anti-rabbit IgG Alexa Fluor 488 at 4 °C for 30 min. Cells were acquired on a Becton Dickinson FACSCalibur flow cytometer (Becton Dickinson, New Jersey, NY, USA). Dead cells were excluded from the analysis using propidium iodide staining (10 μg/mL). The data derived from 5×10^4 cells were analyzed using CellQuest Pro v.5.1 software (Beckton Dickinson). For flow cytometry analysis, the medians of the fluorescence intensity derived from three independent cultures on every culturing day were compared.

2.8. Imaging

Digital images from DIV7, DIV14, and DIV21 cultured primary mixed neuronal cultures were captured using a Leica fluorescence microscope (Leica DMLB; Leica Microsystems, Wetzlar, Germany). To measure the area (μm^2), the perimeter (μm), and the transformation index (TI) of the microglia cells, images were converted into binary replicas using the thresholding procedures implemented in ImageJ, as described previously (Szabo and Gulya, 2013, Kata et al., 2016). For the computation of semi-quantitative cell silhouette characteristics (digital binary pictures), data from 30 cells derived from at least three separate experiments for each culturing time were used. The Ti was determined according to the

Table 1
Antibody final concentrations in flow cytometry staining reactions.

AB	dilution	company	cat#
CD11b	1:50	BD Transduction Laboratories	561,684
CD40	1:500	BD Transduction Laboratories	563,638
CD103	1:150	BD Transduction Laboratories	565,286
Siglec-H	1:50	BD Transduction Laboratories	747,668
CD14	1:50	BD Transduction Laboratories	567,732
RT1A	1:50	BD Transduction Laboratories	745,933
GAL-1	1:50	R and D Systems	IC1245P

following formula: Ti = [perimeter of cell (μm)]^2/4π [cell area (μm^2)]. Ti is a characteristic of the activation state of the cells; a small Ti value (Ti ≤ 2) indicates the amoeboid, activated phenotype of microglial cells (Fujita et al., 1996).

For the comparison of the fluorescence intensity derived from activated and non-activated cells, the observed cells were selected manually in Leica LasX software and the fluorescence intensity mean value of the selected area in the Gal-1 labelled channel were determined. The area and the perimeter of the selected area were measured in Image J and after Ti calculation Gal-1 caused fluorescence mean value from the activated (Ti<2) and the non-activated (Tigreater than2) cells were compared.

Representative images from the branched and amoeboid cells were taken by Leica Stellaris confocal microscope. In the representative measurement presented in Supplemetary Fig. 2, the confocal z-stack has been processed in IMARIS 10.0.1 version software, with background subtraction and 3D segmentation. The cell's soma has been segmented and the red staining intensity has been measured in 3D and normalized for um^3.

2.9. Statistical analysis

Morphometrical comparisons were conducted using Kruskal-Wallis one-way analysis of variance (ANOVA) on rank tests, followed by Tukey's post hoc test, utilizing the Sigma Plot software (v.12.3; Systat Software Inc., Chicago, IL, USA). Statistical comparisons between the number of Gal-1 expressing cells at different timepoints were performed using Kruskal-Wallis ANOVA on ranks, followed by Dunn's method for pairwise multiple comparisons of differences between groups. Western blot data were analyzed in Sigma Plot using Kruskal-Wallis ANOVA on ranks, followed by either Tukey's post hoc test or Student's *t*-test. Flow cytometry data were analyzed in Sigma Plot using one-way ANOVA, followed by Holm-Sidak's method for pairwise multiple comparisons of differences between groups. The results were presented as the mean ± standard error of the mean (SEM). The fluorescence intensity mean value derived from Gal-1 in amoeboid and ramified cells was compared using the Mann-Whitney Rank sum test. A p-value of <0.05 was considered statistically significant.

3. Results

3.1. In silico single-cell analysis revealed a separate microglia population with increased Gal-1 expression in aged mouse brain

To identify Gal-1-expressing microglia in aging brain tissue, the expression pattern of *Gal-1* mRNA was compared between previously published young and aged animal-derived single-cell RNA-seq data (Ximerakis et al., 2019). Cell-type specific gene expression patterns were utilized from the original study. After an initial quality control analysis, a total of 3,885 microglia cells (1,651 from young animals and 2,234 from aged animals) were selected for further analysis. The selected microglia cells were subjected to sub-clustering using the Seurat workflow graph-based algorithm (Stuart et al., 2019), treating all cells as one batch regardless of age. The unsupervised clustering of microglia cells revealed the presence of six distinct sub-clusters with unique gene expression patterns (Fig. 1A). While all sub-clusters were present in both age groups, there was a significant shift in the distribution of cells belonging to different sub-clusters with aging. Specifically, sub-clusters #1 and #5 predominantly consisted of cells from young animals, whereas sub-clusters #0, #2, #3, and #4 were overrepresented in aged animals (Fig. 1B).

Interestingly, Gal-1 mRNA expression was almost exclusively detected in sub-cluster #4, which was predominantly observed in the aged brain (Fig. 1C & D). To assess the statistical significance of the relationship between sub-cluster membership and Gal-1 positivity, a chi-square test of independence was performed. The analysis revealed a significant association between these variables, with X^2 (6, N = 3,885) = 226.25 and a p-value < 2.2e-16.

The analysis of differential gene expression utilizing the Wilcoxon Rank Sum test has revealed the identification of 304 genes that exhibit significant differences within cluster 4 when compared to the remaining microglia clusters. This information can be found in Supplementary Table 1.

Furthermore, the Gene Ontology overrepresentation analysis has shed light on the functional associations of the differentially expressed genes within cluster 4. Notably, these genes are associated with mitochondrial function, cytokine production, and TNF-alpha production. This valuable insight is documented in Supplementary Table S2.

In the sub-cluster #4 the only RNA derived from immune regulatory gene, which expressed almost double level in a quite visible cell population (around 25 % of the cells) was the Gal-1 RNA (circled in Fig 1E). The other activation related RNAs like CD40 (TNF receptor subfamily member 5), CD206 (Mrc1, mannose receptor) CD163 (scavanger receptor) were presented very few number of cells or expressed in decreased level like SiglecH (sialic acid receptor), CD14 (myeloid specific leucine rich glycoprotein) and CD16 (Fcgr3, Fc gamma receptor III) RNAs (Fig 1E.).

Furthermore, a comparative analysis was conducted on a human microglia population obtained from a brain affected by Alzheimer's disease, using the same computational methods employed for the mouse brain analysis (Alsema et al., 2020). However, the expression differences observed in the human microglia population were not as distinct as those observed in the mouse microglia population. Nonetheless, a distinct subpopulation of microglia characterized by an increased expression of Gal-1 was clearly identifiable (referred to as cluster 0 in Supplementary Fig. 1 A-C).

Despite certain similarities, there were notable differences in the gene expression profiles of this Gal-1 expressing subpopulation of microglia in the Alzheimer's-affected human brain. Specifically, the gene expression alterations that distinguished this subpopulation from other microglia subpopulations primarily centered around mitochondrial genes, with no significant deviations observed in the expression of TNF and TNF-related cytokine genes (as depicted in Supplementary Fig. 1 D).

3.2. Gal-1 protein expression in microglial cells is decreased during cultivation and is coupled to LPS-induced activation

Western blotting analyses were conducted on primary cultures at various time points, revealing a gradual decrease in the expression of the Gal-1 protein by DIV21 (Fig. 2A). To investigate activation-associated Gal-1 expression, microglia-enriched cultures were treated with the immune activator bacterial LPS, which resulted in an increase in Gal-1 protein expression (Fig. 2B).

3.3. The activatory molecules and even Gal-1 expression decreased during in vitro culturing of microglial cells

Based on our flow cytometric data obtained from microglial cells derived from mixed cortical cultures at DIV7, DIV14, and DIV21 (as detailed in Fig 3), several conclusions can be drawn. Firstly, the ratio of CD11b expressing cells exhibited a continuous but non-significant decrease over the culturing time (Fig 3 A-B-C). Secondly, the percentage of CD40 expressing cells showed an initial increase during the early period of culturing (until DIV7), followed by a substantial decrease at DIV14 and DIV21 (Fig 3 D-E-F). Furthermore, the number of Gal-1 expressing cells significantly decreased compared to the starter culture (Fig 3 G-H-I). Likewise, the number of Siglec-H positive cells decreased, with a particularly drastic decrement observed between DIV14 and DIV21 (Fig 3 J-K-L). Interestingly, the number of CD14 expressing cells remained unchanged throughout the culturing process (Fig 3 M-N-O). Additionally, the number of RT1A expressing cells decreased over time (Fig 3 P-Q-R).

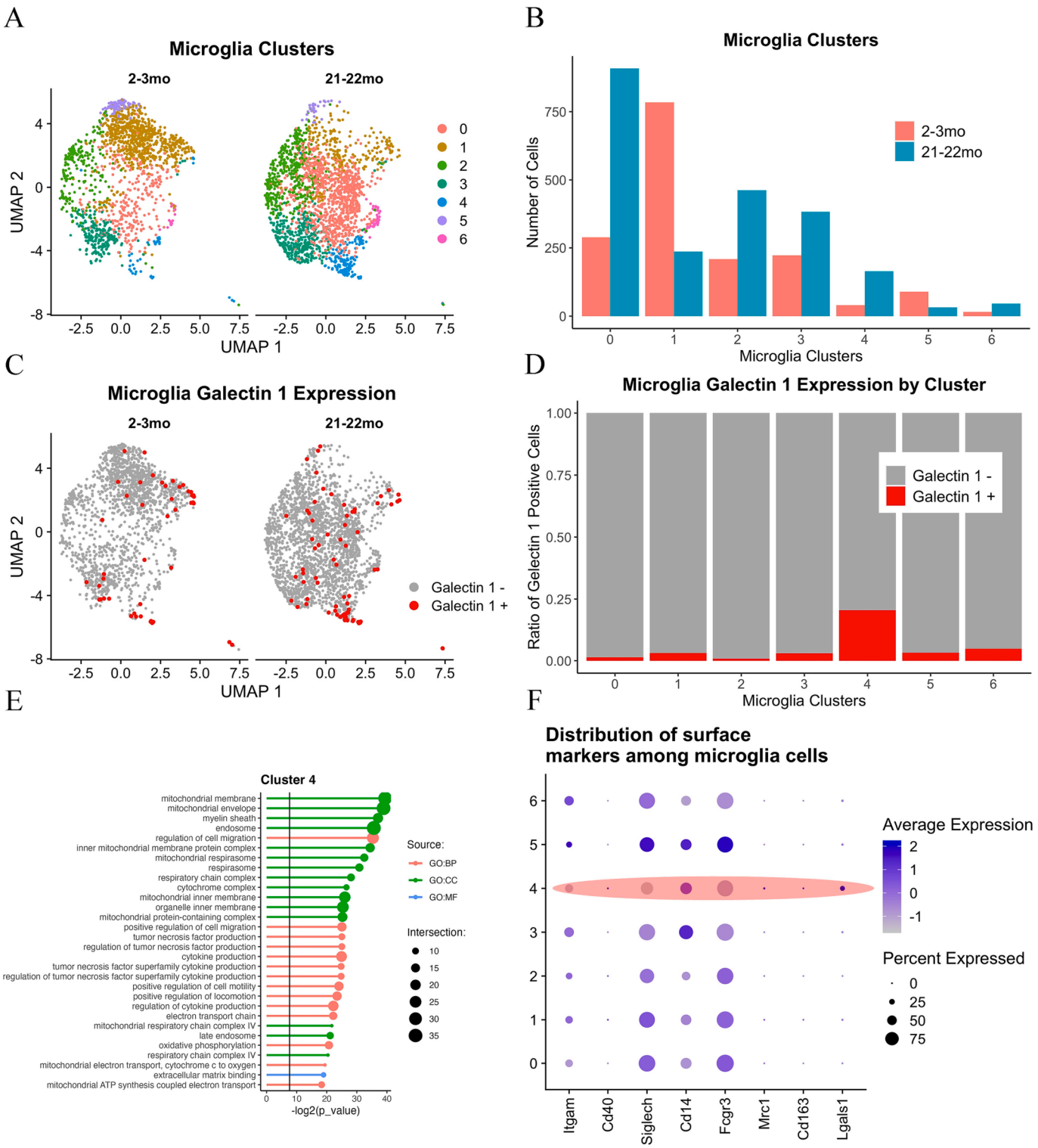

Fig. 1. Analysis of a mouse brain single-cell RNA-seq dataset revealed a distinct sub-cluster of Gal-1-expressing microgila in aged mouse brain. (A) UMAP representation of microglia gene expression by age. Unsupervised clustering of microglia isolated from young (2 to 3 months old, 2–3mo) and aged (21 to 22 months old, 21–22mo) animals identified six distinct sub-clusters. The cells were processed as one batch regardless of age. All sub-clusters were present in both age groups; however, the number of cells belonging to the different sub-clusters showed a significant shift with aging. (B) In young animals, cells belonged to sub-clusters #1 and #5, while in aged animals, cells belonging to sub-clusters #0, #2, #3, and #4 were overrepresented. (C, D) Plotting of the Gal-1-expressing cells in aged animals showed an accumulation almost exclusively in cluster 4. To test the statistical significance between sub-cluster and Gal-1 positivity, a chi-square test of independence was performed. X^2 (6, N = 3885) = 226.25, p-value $<2.2e^{-16}$. (E) Top 30 Gene Ontology terms associated wiht genes differentially expressed in the clustor 4. (F) Analysis of the activation coupled molecules in the microglia sub-clusters revealed that the age related sub-cluster#4 contains exhuasted type of microglial cells with increased Gal-1 expression. In that subgroup almost 25 % percent of the cells express Gal-1 RNAs in an increased level.

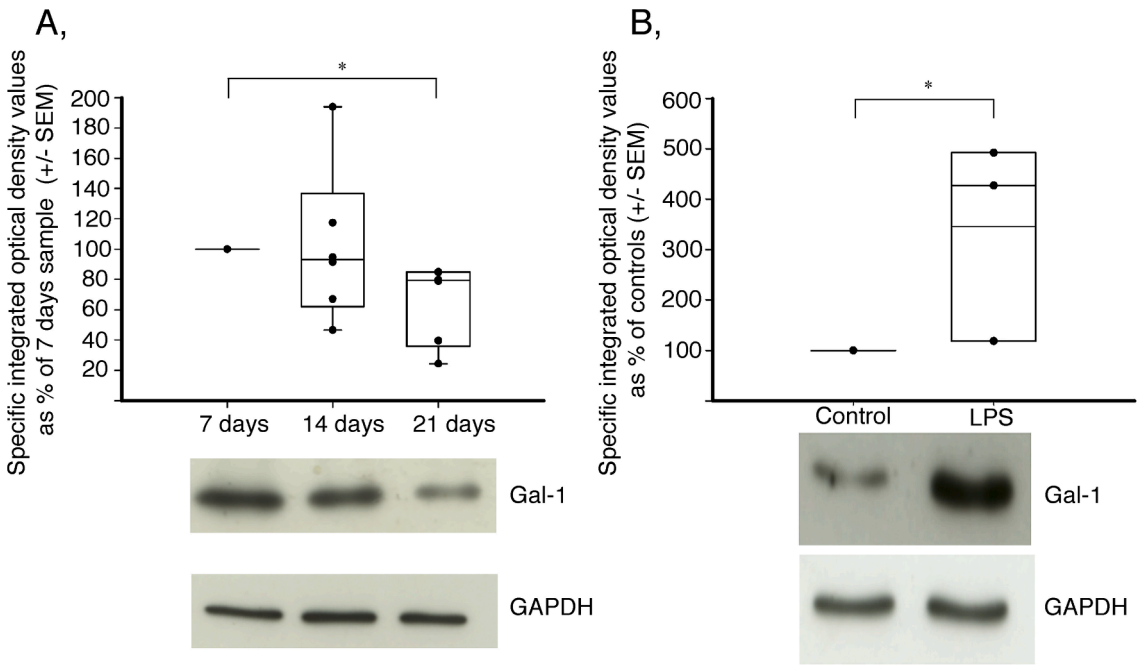

Fig. 2. The activation state of the microglia was coupled with its Gal-1 protein expression. (A) Gal-1 protein expression was decreased during 21 days of culture. The cells from rat primary mixed neuronal cultures were collected from DIV7, DIV14, or DIV21 cultures, lysed, and the Gal-1 protein content of the samples was analyzed with Western blot. The integrated optical density of the Gal-1 protein was quantified with the ImageJ program, then it was normalized with GAPDH expression. The Gal-1 protein level measured at DIV7 was set as a baseline. Data were analyzed with Kruskal–Wallis ANOVA on ranks, followed by Tukey's post hoc test ($n = 6$, $p < 0.05$). Values are presented as the mean ± SEM. (B) LPS promotes Gal-1 expression in microglia-enriched cell cultures. Microglia cultures were prepared from rat primary mixed neuronal cells by vigorous shaking of the cultures. The floating cells were plated for 5 days, then treated with 20 ng/mL LPS at 37 °C for 24 h. The cells were then collected and lysed, and the Gal-1 protein content was quantified by Western blot. The integrated optical density of the Gal-1 bands was measured with the ImageJ program and compared to the non-treated control as a baseline. The intensities of the Gal-1 bands in the LPS-treated samples were higher than those in the non-treated samples, suggesting that Gal-1 expression is coupled to the activated phenotype of microglial cells. The data were analyzed with Student's *t*-test ($n = 3$, $p < 0.05$). Values are presented as mean ± SEM.

3.4. Flow cytometry revealed that part of the expressed Gal-1 was present on the cell surface

The cellular localozation of Gal-1 within microglia was evaluated by examining the binding of an anti-Gal-1 antibody to the Gal-1 protein localized on the cell surface of microglial cells (Fig. 4A). Flow cytometry analysis demonstrated that the Gal-1 protein was detected on the cell surface of isolated amoeboid microglial cells, regardless of whether they were derived from the DIV7, DIV14, or DIV21 time points (Fig. 4B).

3.5. Gal-1-expressing microglia were presented for shorter culturing times and showed activated, amoeboid morphology

To assess the activation status of Gal-1-expressing microglial cells, mixed primary neuronal cultures from rats were prepared. The co-expression of Gal-1 and CD11b/c (OX42) in microglial cells was examined at three different time points. Immunological and morphological parameters of microglial cells were analyzed during the early log phase (DIV7), middle log phase (DIV14), and plateau phase culture (DIV21). A total of thirty slides from each time point, derived from three independent experiments, were examined. The ratio between OX42/Gal-1 double positive cells and OX42-positive/Gal-negative cells exhibited a significant change between DIV14 and DIV21. At DIV7, 95.8% of the cells showed co-expression of OX42 and Gal-1, while at DIV14, this percentage decreased to 70%. Finally, at DIV21, only 10.5% of the cells were positive for both OX42 and Gal-1. Multicolor fluorescent immunocytochemistry revealed that the loss of Gal-1 expression was accompanied by morphological changes. The microglial cells transformed from an amoeboid shape into a ramified, branched appearance, indicative of their exhaustion state after intense phagocytic clearance of injured cells. Importantly, these morphological changes were inversely correlated with the level of Gal-1 expression (Fig. 5A–L).

The area, perimeter, and Ti (shape index) of OX42 (CD11b/c)-positive cells, which serve as indicators of microglia activation, were quantified (Fig. 6A). Our morphological analysis revealed that the area, perimeter, and Ti were significantly greater in OX42-positive microglial cells obtained from DIV21, compared to OX42/Gal-1 double-positive cells from DIV7, DIV14, or even the Gal-1-expressing subpopulation from DIV21 (Fig. 6B, C, & D).

Our representative confocal microscopic images obtained from DIV21 illustrate that the OX42/Gal-1 double-positive microglial cells exhibit an amoeboid morphology, while the Gal-1 non-expressing cells display a distinct branched morphology (Fig. 7 A-I). Furthermore, the fluorescence intensity of Gal-1 was significantly higher in non-activated, amoeboid cells with a shape index (Ti) <2, compared to the branched ramified microglial cells with a TI greater than 2 (Fig. 7 J). To enhance the credibility of our findings, a representative measurement was conducted. This measurement involved comparing the fluorescence signal induced by Gal-1 in highly branched (ramified) cells to that in amoeboid cells, utilizing a z-stacked 3D image (as depicted in Supplementary Fig. 2A-F). The analysis of Gal-1-triggered volume-optimized fluorescence intensity revealed that amoeboid cells exhibited an approximately 50% higher intensity compared to the control ramified cells (as illustrated in Supplementary Fig. 2F).

4. Discussion

Neurodegenerative diseases and aging are often associated with chronic inflammatory processes. The primary regulators of immune homeostasis within the central nervous system (CNS) are microglial cells. These cells secrete factors that contribute to maintaining tissue balance in the brain. Under normal conditions, microglial cells exhibit a

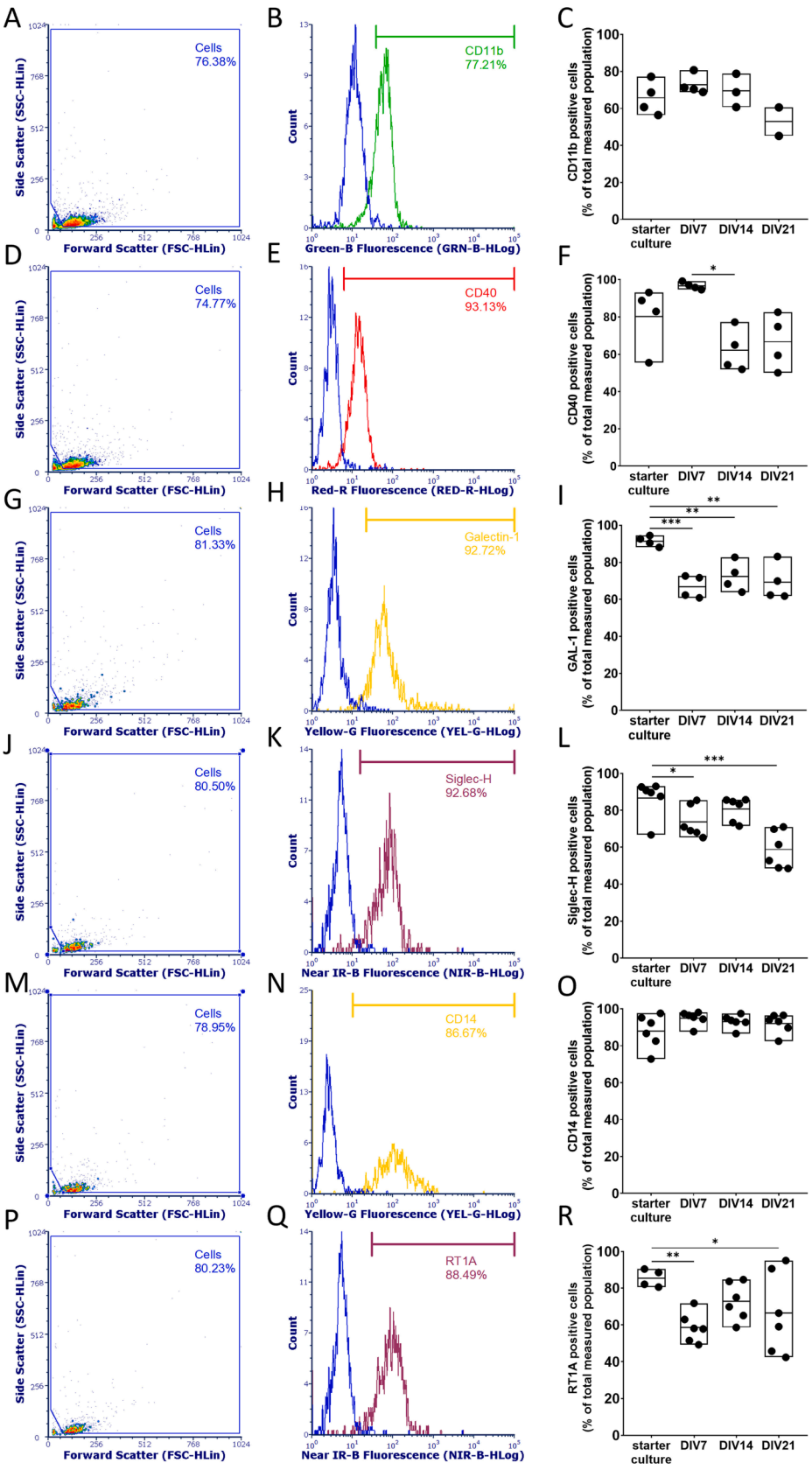

Fig. 3. Galectin-1 protein expression level predicts microglia activation and exhaustion. Microglia cell type and activity markers have been stained and intensity-based measurement of the cells has been assessed with quantitative flow cytometry. A) Representative panels show that cellular debri and other non-cellular components have been gated out and only whole cells were measured. B) Representative panels about the gating strategy for the marker proteins labeling on starter, DIV7, 14, and 21 cultures. C) Quantification of cell populations labelled with different cell type and activity markers. Note the reducing numbers of the activity marker positive populations and also GAL-1 positive cells with time. Data were analyzed with one-way ANOVA followed by Fisher LSD method (n = 3–6, *p < 0.05; **p < 0.01; ***p < 0.001). Values are presented as the mean ± SEM.

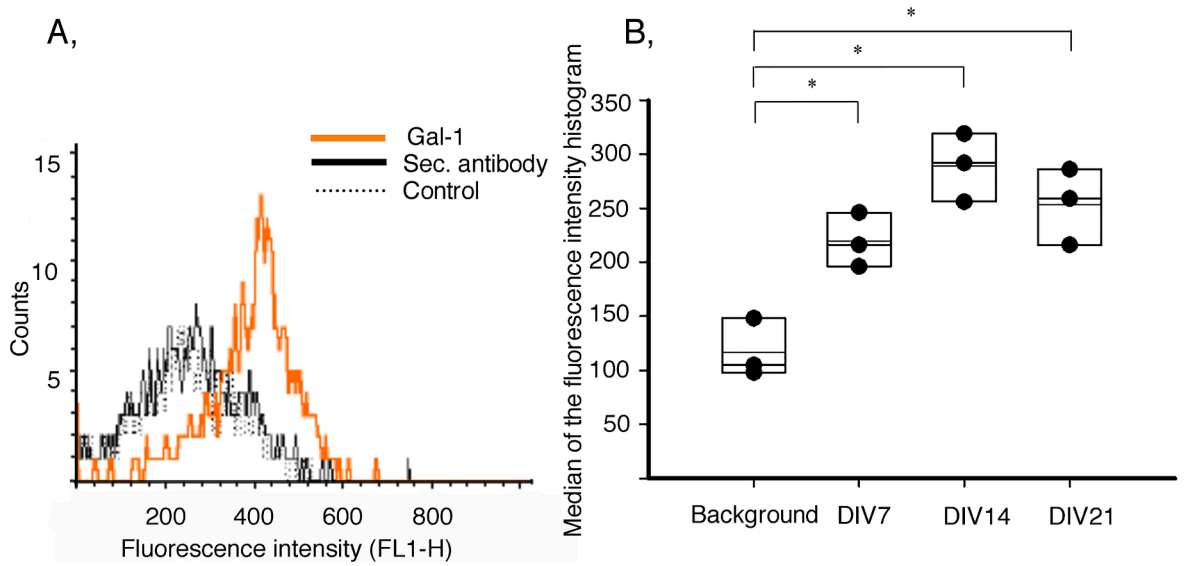

Fig. 4. Gal-1 protein is present on the cell surfaces of microglia. (A) Microglial cells were isolated from DIV7 rat primary mixed neuronal cell cultures. Cell surface-bound Gal-1 was labeled with rabbit anti-Gal-1 antibody at 4 °C and anti-rabbit IgG Alexa Fluor 488. Fluorescence intensity derived from the cell surface-bound Gal-1 was increased, as shown in the histogram, after measurement of 5×10^4 cells by flow cytometry (B) Gal-1 antibody-derived immunofluorescence was present in the microglia cells isolated from DIV7, DIV14, and DIV21 primary cultures. The median of the fluorescence intensity histogram was significantly increased in the DIV7, DIV14, or DIV21 primary mixed neuronal culture-isolated microglial cells compared with the background non-labeled control microglial population. Data were analyzed with one-way ANOVA followed by Holm–Sidak's method ($n = 3$, $p < 0.05$). Values are presented as the mean ± SEM.

ramified morphology and display subdued functional properties similar to macrophages. However, in response to neural injury or infection, microglia undergo activation, leading to various morphological, molecular, immunological, and functional changes (Kreutzberg, 1996; Town et al., 2005).

During the aging process, almost all functions of microglia undergo alterations. Microglia exhibit features of senescence (Streit and Xue, 2013), impaired phagocytic and movement capacities (Ritzel et al., 2019), and changes in their protostatic functions, signaling capacity, and morphology (Damani et al., 2011). These age-related changes contribute to the altered functionality of microglia in the aging brain.

Single-cell analysis-based data have provided insights into the complex gene expression patterns of microglia, revealing significant changes during the aging process (Galatro et al., 2017). Through our in silico single-cell analysis, we identified a distinct microglial population characterized by a significant enrichment of Gal-1 expression, which is a hallmark of the aged mouse brain. Aging is closely associated with neuroinflammation, a process that plays a critical role in the development of neurodegenerative diseases such as Alzheimer's and Parkinson's diseases (Ownby, 2010; López-Otín et al., 2013; Conde and Streit, 2006).

During the aging process, there is an increase in the levels of inflammatory cytokines such as IL-1 and IL-6, which contribute to neuroinflammation. Additionally, evidence suggests that certain anti-inflammatory cytokines, including TGF and ILRa, also exhibit elevated levels (Forsey et al., 2003; Cavallone et al., 2003; Minciullo et al., 2016). These changes in cytokine levels further contribute to the inflammatory milieu associated with aging and its impact on the CNS.

In vitro cultivation of microglial cells has been widely utilized as a well-established model to study and compare the expression patterns of activated amoeboid and inactivated ramified microglial cells. In mixed cultures, the morphology of microglia cells undergoes continuous transformation from an amoeboid to a ramified state between DIV10 and DIV28, primarily driven by the extensive loss of neurons. This dynamic process is attributed to the presence of neuronal cell debris in the culture environment, which triggers overactivation of microglial cells (Szabo and Gulya, 2013; Amur-Umarjee et al., 1990).

These morphological changes are accompanied by profound alterations in the gene expression patterns of microglia, leading to a state of exhaustion and reduced responsiveness to antigens. During the amoeboid stage, microglia retain intact phagocytic activity and immune function associated with HLA-DP, -DQ, and -DR proteins. However, it has been observed that prolonged culture duration can lead to a decline in NF-kB activation and the expression of toll-like receptor 2 and 4 (Caldeira et al., 2014). These changes suggest that long-term culture conditions can impact the activation status and immune-related functions of microglial cells, potentially influencing their ability to respond to inflammatory stimuli.

Our hypothesis posits that the depletion of Gal-1, a well-characterized member of the galectin family known for its anti-inflammatory properties, may contribute to the emergence of a refractory microglial phenotype.

Concurrently with the increase in the number of microglial cells throughout the culturing period in the primary mixed neuronal culture (Szabo and Gulya, 2013), the level of Gal-1 within the culture exhibited a decrement, suggesting a correlation between Gal-1 expression and microglial activation state. The administration of LPS, a commonly used immunostimulant known to induce the expression of tolerogenic signaling molecules and Gal-1 in bone marrow-derived dendritic cells (Zhou et al, 2014), confirmed the activation-dependent expression of Gal-1. This was further supported by Western blot analysis, which demonstrated an elevated level of Gal-1 in microglia-enriched cultures upon exposure to LPS. Our comprehensive immunocytochemistry-based investigation also substantiated that Gal-1 expression was linked to the amoeboid activated morphology of microglial cells rather than the ramified cells.

Prior investigations have elucidated the involvement of beta-galactoside-binding lectin, specifically Gal-1, in the cellular immune response in various tissues (Perillo et al., 1995). In the context of autoimmune neuroinflammation, the exogenous addition of Gal-1 has demonstrated neuroprotective effects by preventing neurodegeneration and inducing microglial deactivation, thereby activating their neuroprotective functions (Starossom et al., 2012).

While Gal-1 can be found intracellularly (Liu et al., 2002; Park et al., 2001) and extracellularly, the majority of its biological functions are associated with its membrane-bound, extracellular form (Camby et al., 2006). Our findings indicate that a subset of microglial cells expresses

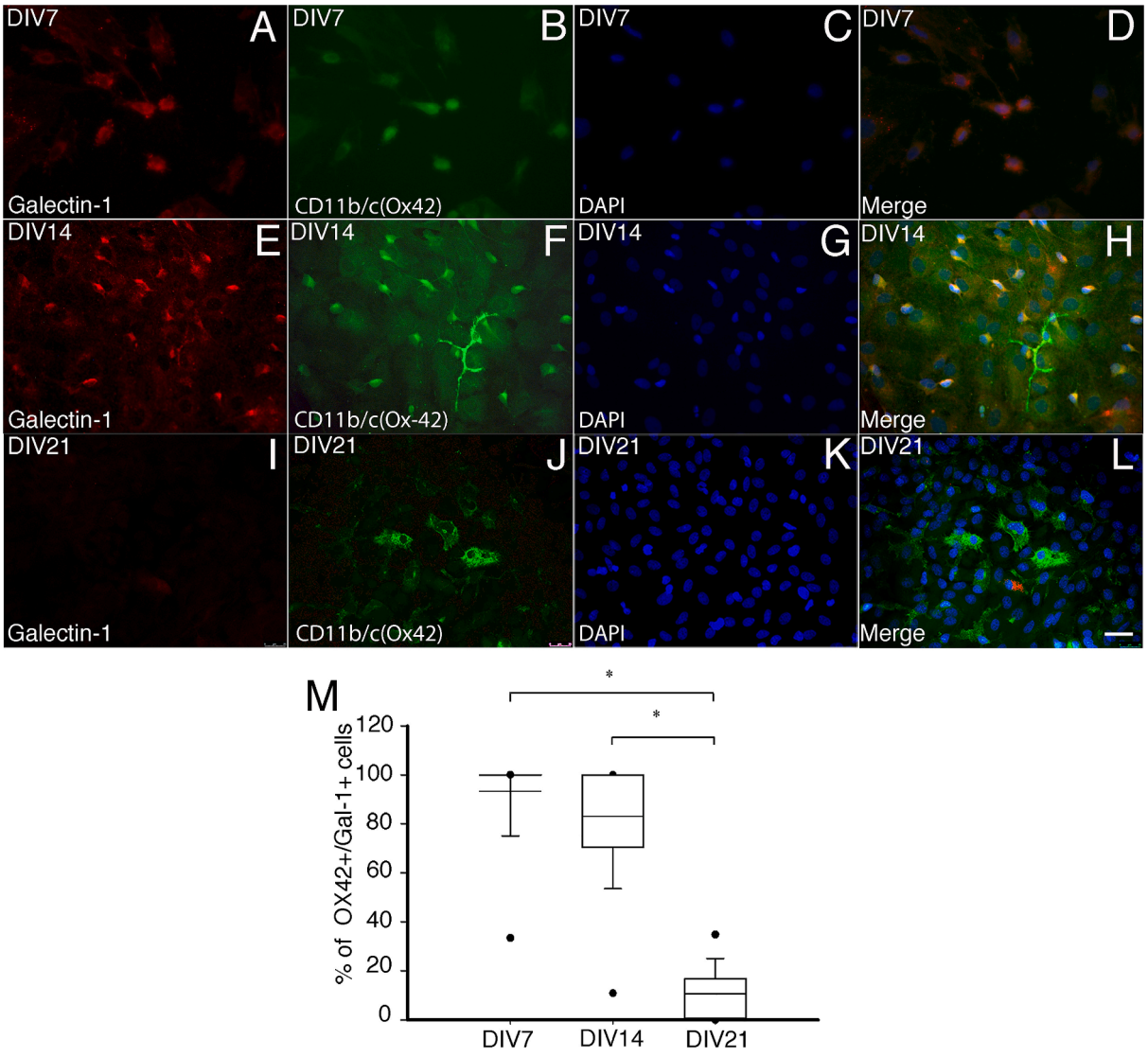

Fig. 5. CD11b/c -expressing microglia cells (DIV21) displayed branched morphology and were devoid of the Gal-1 expression. Primary mixed neuronal cell cultures derived from newborn rats were plated and cultured for 7, 14, or 21 days (DIV7, DIV14, or DIV21). Cells were fixed, and Gal-1 protein was labeled with rabbit anti-Gal-1 antibody and visualized with anti-rabbit IgG Alexa Fluor 568 (red, A, E, and I). CD11b/c-positive microglial cells were labeled with mouse anti-CD11b/c (OX42) antibody and anti-mouse IgG Alexa Fluor 488 (green, B, F, and J). Nuclei were labeled with Hoechst dye (C, G, and K). Scale bar: 25 μm. M) The OX42+ and the Ox42+/Gal+ microglial cells were counted on 30 slides derived from three independent cultures at all culturing time points. The percentage of OX42+/Gal-1+ from total OX42+ microglial cells decreased dramatically until DIV21.Statistical analysis were performed with using one-way ANOVA followed by Dunns's method for pairwise multiple comparisons of differences between ($n=30$, $p < 0.05$). Values are presented as mean ± SEM. (For interpretation of the references to colour in this figure legend, the reader is referred to the web version of this article.)

Gal-1 on their cell surface. Gal-1 exhibits a strong affinity for its ligands (He and Baum, 2006; Fajka-Boja et al., 2016). Notably, cell surface-localized Gal-1 on tumor cells has been shown to induce cell death in activated T cells more effectively than the soluble form of Gal-1 (Kovács-Sólyom et al., 2010). Carbohydrate recognition molecules that are bound to the cell surface play a crucial role in regulating microglial activation since microglial cells continually monitor the glycosylation patterns of neighboring cells using their cell surface-bound carbohydrate recognition proteins. Removal of the terminal sialic acid structure triggers microglial activation through the immunoreceptor tyrosine-based activation motif-coupled activation of complement receptors, thereby enhancing the binding affinity of Gal-1 to the desialylated glycan structure (Schnaar, 2004; Linnartz and Neumann, 2013; Linnartz et al., 2012).

5. Limitations

This study possesses several limitations that necessitate careful consideration when interpreting the findings. Firstly, although there are notable similarities in the gene expression patterns of microglia between humans and rodents (evidenced by shared expression levels of Iba-1, DAP12, MCSF-receptors, among others), it is crucial to recognize the significant differences in gene expression (such as the presence of syalic acid binding lectin, Siglecs, exclusively in humans) and inflammatory response reactions. These disparities hinder the clinical applicability of experimental data derived from rodent microglia (Smith and Dragunow, 2014). Consequently, these differences play a significant role in explaining the discrepancies observed in gene annotation studies between humans and mice, underscoring the importance of parallel utilization of human and rodent experimental data.

Secondly, while standard statistical methods were employed during

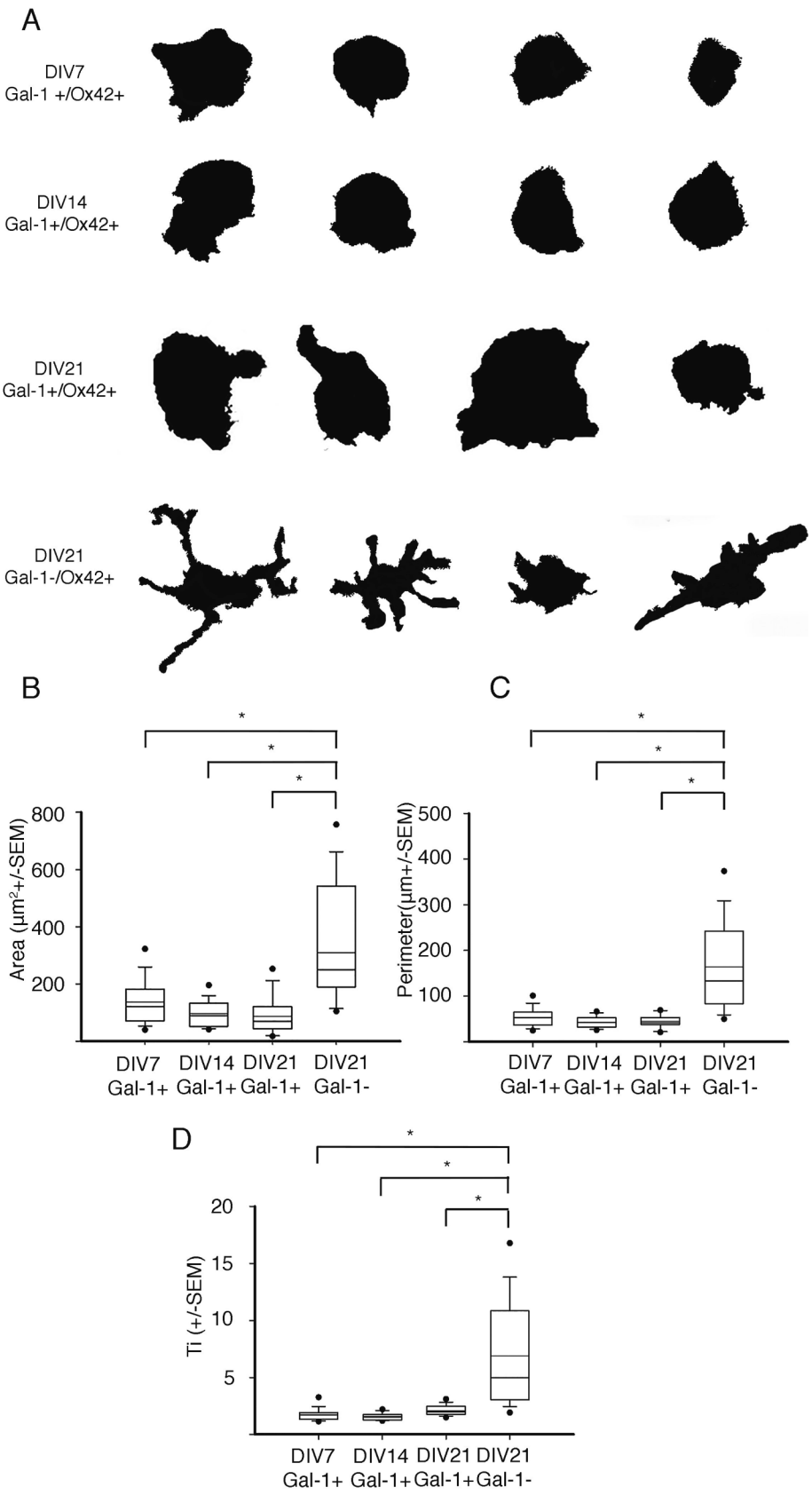

Fig. 6. Quantitative analysis of cultured microglia indicated that the cell area, perimeter, and TI values increased during replicative aging as the cells became more ramified (DIV21). These branched, ramified cells were negative for Gal-1 antigen. The cell images of 30 cells derived from three independent cultivations were transformed into binary replicas (silhouettes) using automatic thresholding procedures (A). The area (B) and the perimeter (C) of the binary silhouettes were measured using ImageJ. From these data, the Ti value (D) was calculated (TI = perimeter $(\mu m)^2/4\pi$ cell area (μm^2)). Smaller Ti values at DIV7. DIV14 and DIV21 indicated amoeboid and activated cell phenotype, and higher Ti values at DIV21 indicated that microglial cells had lost their activation status during the long culturing time. Statistical analyses were performed with one-way ANOVA on ranks, followed by Tukey's post hoc test ($p < 0.05$). Values are presented as mean ± SEM.

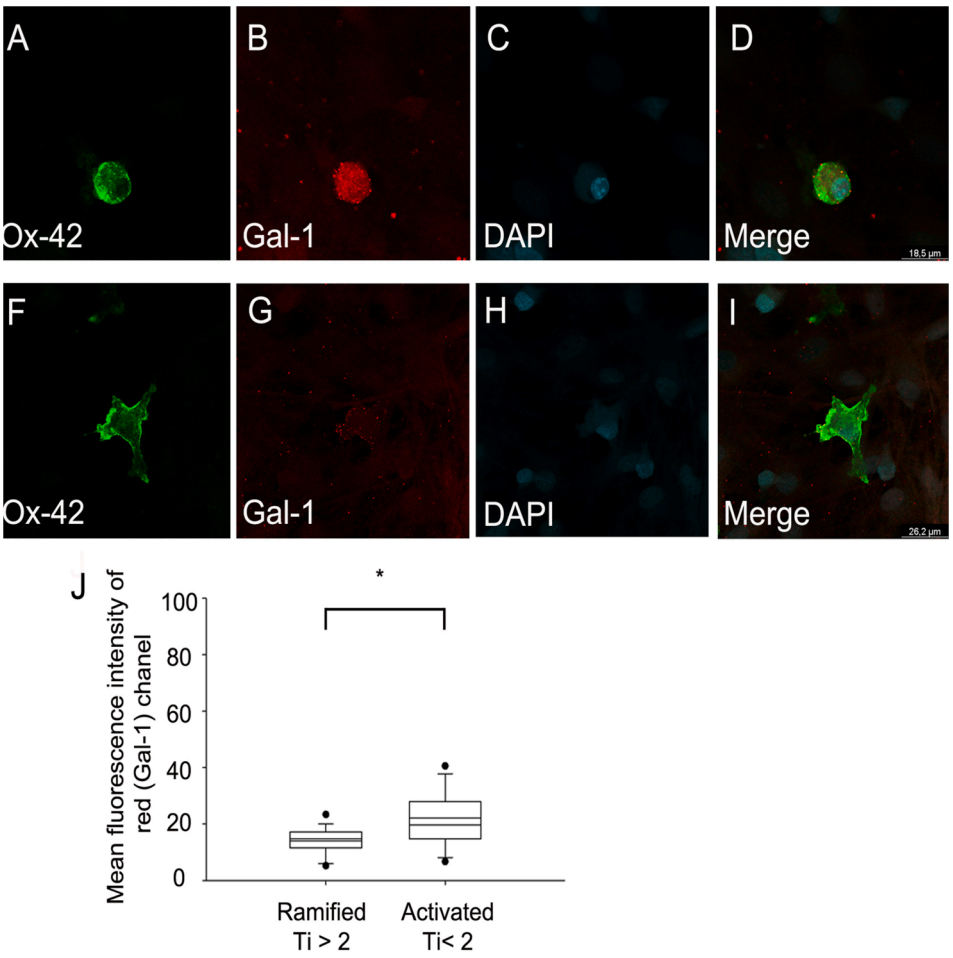

Fig. 7. The Gal-1 positive microglial cells shows amoeboid morphology and express more Gal-1. The Cd11b/c and Gal- proteins in the microglial cells derived from primary mixed culture at DIV21 were labelled with rabbit derived polyclonal anti-Gal-1 and mouse derived anti-CD11b/c (Ox42) antibodies. The bound antibodies were visualized with the help of Alexa 488 conjugated anti mouse IgG (green, A, I) and Alexa 568 conjugated anti-rabbit IgG (red, B and G). The cell nuclei were labelled with DAPI (blue, C and H). The pictures were taken by Leica Stellaris confocal microscope. J, Ti number from at least 200 Gal-1 and Ox42 labelled cells were determined, and the fluorescence intensities of Gal-1 derived channel were compared from the amoeboid (Ti<2) and the ramified cells (Tigreater than2) cells. The data were analyzed with Man-Whitney Rank sum test (p< 0,05). Values are presented as mean ± SEM. (For interpretation of the references to colour in this figure legend, the reader is referred to the web version of this article.)

the in silico single-cell RNASeq analysis, it is imperative to acknowledge that the clustering of cells heavily relies on the specific configuration of the statistical system. Even minor adjustments to the setup can yield distinct clustering patterns among cell populations.

Thirdly, although long-term cultivation of cells can induce gene expression changes reminiscent of cellular senescence (Caldeira et al., 2014), it is worth noting that the primary cells used in the in vitro experiments were obtained from newborn rats. Therefore, their genetic status may not directly correspond to that of aged microglia in vivo.

The fourth limitation concerns the experimental procedures employed, which did not permit direct assessment of Gal-1′s functional role. No actual functional tests were conducted to evaluate the regulation of Gal-1 secretion or the consequences of Gal-1 binding to nervous tissue cells. Thus, while the results clearly indicate that morphologically active amoeboid microglial cells express Gal-1, the specific functional implications of this Gal-1 expression within the context of aging conditions and its effects on microglial populations remain to be elucidated.

Lastly, despite the noticeable differences in Gal-1-induced fluorescence signal intensity observed between amoeboid and ramified cells using widefield and confocal microscopic systems, it is essential to consider that comparing fluorescence intensity signals may not accurately convey information about the total signal amount in cells with distinct morphologies and volumes.

Given these limitations, the present study proposes that Gal-1 expression acts as a bystander effect in aging conditions within a specific population of microglial cells. However, further investigations are warranted to fully comprehend the functional implications and significance of Gal-1 in microglial biology.

6. Conclusion

The delicate equilibrium between pro-inflammatory and anti-inflammatory signals plays a crucial role in dictating the progression of various diseases characterized by inflammation with relapsing-remitting phenotypes, such as multiple sclerosis (Lublin et al, 2014). However, this balance becomes disrupted during the neuro-inflammatory processes associated with aging. In accordance with our hypothesis, not only the expression of anti-inflammatory cytokine-like molecules undergoes changes during microglial activation but also the presence of immunoregulatory carbohydrate-binding molecules, such as Gal-1. Remarkably, Gal-1 expression selectively marks microglial populations associated with aging in the brain. Furthermore, the expression of Gal-1 is linked to the activated phenotype of microglial cells. Our findings, in concordance with existing literature, suggest that Gal-1-expressing activated microglia may play a significant role in regulating neuroinflammation associated with aging and the development of age-related neurodegenerative disorders. Consequently, the modulation of Gal-1 expression in the microglial population within the aging brain represents a promising therapeutic target for mitigating neurodegenerative processes (Li et al., 2020).

Ethical approval

All applicable international, national, and/or institutional guidelines for the care and use of animals were followed. Experimental procedures were carried out in strict compliance with the European Communities Council Directive (86/609/EEC) and followed Hungarian legislation requirements (XXVIII/1998 and 243/1998) and university guidelines

regarding the care and use of laboratory animals. All experimental protocols were approved by the Institutional Animal Welfare Committee of the University of Szeged (II./1131/2018).

Funding information

This work was supported by a grant from EFOP-3.6.1-16-2016-00008 and GINOP-2.3.2-15-2016-00034 grants. ANyT was supported by American Heart Association (AHA834339). (The funders had no role in the study design, data collection and analysis, decision to publish, or preparation of the manuscript). This research was funded by the 2020-1.1.6-JÖVŐ−2021-00003 and 142877 FK22, grant from the National Research, Development, and Innovation Office (NKFI), Hungary. This work was supported by the ÚNKP-22-5 -SZTE-535 New National Excellence Program (GJS) of the Ministry for Innovation and Technology from the source of the National Research, Development and Innovation Fund. This work was supported by the János Bolyai Research Scholarship of the Hungarian Academy of Sciences BO/00582/22/8 (GJS).

CRediT authorship contribution statement

Tamas Kiss: Conceptualization, Methodology, Software, Formal analysis, Data curation, Visualization, Writing – original draft, Writing – review & editing. **Yaqub Mir:** Conceptualization, Investigation, Writing – original draft, Writing – review & editing. **Gergely Stefancsik:** Investigation. **Gantulga Ganbat:** Investigation. **Aruzhan Askarova:** Investigation. **Eva Monostori:** Resources. **Karolina Dulka:** Investigation. **Gabor J. Szebeni:** Investigation. **Ádám Nyúl-Tóth:** Investigation, Formal analysis, Visualization. **Anna Csiszár:** Conceptualization. **Adam Legradi:** Conceptualization, Methodology, Validation, Investigation, Writing – original draft, Writing – review & editing, Visualization, Supervision, Project administration.

Declaration of Competing Interest

The authors declare that they have no known competing financial interests or personal relationships that could have appeared to influence the work reported in this paper.

Data availability

No data was used for the research described in the article.

Acknowledgments

We thank Mrs. Edina Ratkai for the excellent technical assistance. We thank for Mr. Dr. Ferhan Ayadin for confocal microscope support.

Appendix A. Supplementary data

Supplementary data to this article can be found online at https://doi.org/10.1016/j.brainres.2023.148517.

References

Alsema, A.M., Jiang, Q., Kracht, L., Gerrits, E., Dubbelaar, M.L., Miedema, A., Brouwer, N., Hol, E.M., Middeldorp, J., van Dijk, R., Woodbury, M., Wachter, A., Xi, S., Möller, T., Biber, K.P., Kooistra, S.M., Boddeke, E.W.G.M., Eggen, B.J.L., 2020. Profiling Microglia From Alzheimer's Disease Donors and Non-demented Elderly in Acute Human Postmortem Cortical Tissue. Front. Mol. Neurosci. 28 (13), 134. https://doi.org/10.3389/fnmol.2020.00134. PMID: 33192286; PMCID: PMC7655794.

Amur-Umarjee, S.G., Dasu, R.G., Campagnoni, A.T., 1990. Temporal expression of myelin-specific components in neonatal mouse brain cultures: evidence that 2,3-cyclic nucleotide 3-phosphodiesterase appears prior to galactocerebroside. Dev. Neurosci. 12 (4–5), 251–262. https://doi.org/10.1159/000111854. PMID: 1963138.

Becht, E., McInnes, L., Healy, J., Dutertre, C.-A., Kwok, I.W.H., Ng, L.G., Ginhoux, F., Newell, E.W., 2019. Dimensionality reduction for visualizing single-cell data using UMAP. Nat. Biotechnol. 37 (1), 38–44.

Blaser, C., Kaufmann, M., Müller, C., Zimmermann, C., Wells, V., Mallucci, L., Pircher, H., 1998. Beta-galactoside-binding protein secreted by activated T cells inhibits antigen-induced proliferation of T cells. Eur. J. Immunol. 28 (8), 2311–2319. https://doi.org/10.1002/(SICI)1521-4141(199808)28:08<2311::AID-IMMU2311>3.0.CO;2-G. PMID: 9710209.

Caldeira, C., Oliveira, A.F., Cunha, C., Vaz, A.R., Falcão, A.S., Fernandes, A., Brites, D., 2014. Microglia change from a reactive to an age-like phenotype with the time in culture. Front. Cell. Neurosci. 2 (8), 152. https://doi.org/10.3389/fncel.2014.00152. PMID: 24917789; PMCID: PMC4040822.

Camby, I., Le Mercier, M., Lefranc, F., Kiss, R., 2006. Galectin-1: a small protein with major functions. Glycobiology 16 (11), 137R–157R. https://doi.org/10.1093/glycob/cwl025. Epub 2006 Jul 13 PMID: 16840800.

Cavallone, L., Bonafè, M., Olivieri, F., Cardelli, M., Marchegiani, F., Giovagnetti, S., Di Stasio, G., Giampieri, C., Mugianesi, E., Stecconi, R., Sciacca, F., Grimaldi, L.M., De Benedictis, G., Lio, D., Caruso, C., Franceschi, C., 2003. The role of IL-1 gene cluster in longevity: a study in Italian population. Mech. Ageing Dev. 124 (4), 533–538. https://doi.org/10.1016/s0047-6374(03)00033-2. PMID: 12714264.

Chung NC, Storey JD. Statistical significance of variables driving systematic variation in high-dimensional data. Bioinformatics. 2015 Feb 15;31(4):545-54. doi: 10.1093/bioinformatics/btu674. Epub 2014 Oct 21. PMID: 25336500; PMCID: PMC4325543.

Conde, J.R., Streit, W.J., 2006. Microglia in the aging brain. J. Neuropathol. Exp. Neurol. 65 (3), 199–203. https://doi.org/10.1097/01.jnen.0000202887.22082.63. PMID: 16651881.

Damani MR, Zhao L, Fontainhas AM, Amaral J, Fariss RN, Wong WT. Age-related alterations in the dynamic behavior of microglia. Aging Cell. 2011 Apr;10(2):263-76. doi: 10.1111/j.1474-9726.2010.00660.x. Epub 2010 Dec 29. PMID: 21108733; PMCID: PMC3056927.

Fajka-Boja, R., Urbán, V.S., Szebeni, G.J., Czibula, Á., Blaskó, A., Kriston-Pál, É., Makra, I., Hornung, Á., Szabó, E., Uher, F., Than, N.G., Monostori, É., 2016. Galectin-1 is a local but not systemic immunomodulatory factor in mesenchymal stromal cells. Cytotherapy 18 (3), 360–370. https://doi.org/10.1016/j.jcyt.2015.12.004. PMID: 26857229.

Forsey, R.J., Thompson, J.M., Ernerudh, J., Hurst, T.L., Strindhall, J., Johansson, B., Nilsson, B.O., Wikby, A., 2003. Plasma cytokine profiles in elderly humans. Mech. Ageing Dev. 124 (4), 487–493. https://doi.org/10.1016/s0047-6374(03)00025-3. PMID: 12714257.

Frasca, D., Blomberg, B.B., 2016. Inflammaging decreases adaptive and innate immune responses in mice and humans. Biogerontology 17 (1), 7–19.

Fujita, H., Tanaka, J., Toku, K., Tateishi, N., Suzuki, Y., Matsuda, S., Sakanaka, M., Maeda, N., 1996. Effects of GM-CSF and ordinary supplements on the ramification of microglia in culture: a morphometrical study. Glia 18 (4), 269–281. https://doi.org/10.1002/(sici)1098-1136(199612)18:4<269::aid-glia2>3.0.co;2-t. PMID: 8972796.

Galatro, T.F., Holtman, I.R., Lerario, A.M., Vainchtein, I.D., Brouwer, N., Sola, P.R., Veras, M.M., Pereira, T.F., Leite, R.E.P., Möller, T., Wes, P.D., Sogayar, M.C., Laman, J.D., den Dunnen, W., Pasqualucci, C.A., Oba-Shinjo, S.M., Boddeke, E.W.G.M., Marie, S.K.N., Eggen, B.J.L., 2017. Transcriptomic analysis of purified human cortical microglia reveals age-associated changes. Nat. Neurosci. 20 (8), 1162–1171. https://doi.org/10.1038/nn.4597. Epub 2017 Jul 3 PMID: 28671693.

Ginhoux F, Greter M, Leboeuf M, Nandi S, See P, Gokhan S, Mehler MF, Conway SJ, Ng LG, Stanley ER, Samokhvalov IM, Merad M. Fate mapping analysis reveals that adult microglia derive from primitive macrophages. Science. 2010 Nov 5;330(6005):841-5. doi: 10.1126/science.1194637. Epub 2010 Oct 21. PMID: 20966214; PMCID: PMC3719181.

He, J., Baum, L.G., 2006. Galectin interactions with extracellular matrix and effects on cellular function. Methods Enzymol. 417, 247–256. https://doi.org/10.1016/S0076-6879(06)17017-2. PMID: 17132509.

Heneka, M.T., Carson, M.J., El Khoury, J., Landreth, G.E., Brosseron, F., Feinstein, D.L., Jacobs, A.H., Wyss-Coray, T., Vitorica, J., Ransohoff, R.M., Herrup, K., Frautschy, S. A., Finsen, B., Brown, G.C., Verkhratsky, A., Yamanaka, K., Koistinaho, J., Latz, E., Halle, A., Petzold, G.C., Town, T., Morgan, D., Shinohara, M.L., Perry, V.H., Holmes, C., Bazan, N.G., Brooks, D.J., Hunot, S., Joseph, B., Deigendesch, N., Garaschuk, O., Boddeke, E., Dinarello, C.A., Breitner, J.C., Cole, G.M., Golenbock, D. T., Kummer, M.P., 2015. Neuroinflammation in Alzheimer's disease. Lancet Neurol. 14 (4), 388–405. https://doi.org/10.1016/S1474-4422(15)70016-5. PMID: 25792098; PMCID: PMC5909703.

Hirabayashi, J., Kasai, K., 1993. The family of metazoan metal-independent beta-galactoside-binding lectins: structure, function and molecular evolution. Glycobiology 3 (4), 297–304. https://doi.org/10.1093/glycob/3.4.297. PMID: 8400545.

Hoeffel, G., Chen, J., Lavin, Y., Low, D., Almeida, F.F., See, P., Beaudin, A.E., Lum, J., Low, I., Forsberg, E.C., Poidinger, M., Zolezzi, F., Larbi, A., Ng, L.G., Chan, J.K., Greter, M., Becher, B., Samokhvalov, I.M., Merad, M., Ginhoux, F., 2015. C-Myb(+) erythro-myeloid progenitor-derived fetal monocytes give rise to adult tissue-resident macrophages. Immunity 42 (4), 665–678. https://doi.org/10.1016/j.immuni.2015.03.011. PMID: 25902481; PMCID: PMC4545768.

Ion, G., Fajka-Boja, R., Kovács, F., Szebeni, G., Gombos, I., Czibula, A., Matkó, J., Monostori, E., 2006. Acid sphingomyelinase mediated release of ceramide is essential to trigger the mitochondrial pathway of apoptosis by galectin-1. Cell. Signal. 18 (11), 1887–1896. https://doi.org/10.1016/j.cellsig.2006.02.007. Epub 2006 Mar 6 PMID: 16549336.

Ishibashi, S., Kuroiwa, T., Sakaguchi, M., Sun, L., Kadoya, T., Okano, H., Mizusawa, H., 2007. Galectin-1 regulates neurogenesis in the subventricular zone and promotes

functional recovery after stroke. Exp. Neurol. 207 (2), 302–313. https://doi.org/10.1016/j.expneurol.2007.06.024. Epub 2007 Jul 17 PMID: 17706645.
Kata, D., Földesi, I., Feher, L.Z., Hackler Jr, L., Puskas, L.G., Gulya, K., 2016. Rosuvastatin enhances anti-inflammatory and inhibits pro-inflammatory functions in cultured microglial cells. Neuroscience 9 (314), 47–63. https://doi.org/10.1016/j.neuroscience.2015.11.053. Epub 2015 Nov 26 PMID: 26633263.
Kata, D., Földesi, I., Feher, L.Z., Hackler Jr, L., Puskas, L.G., Gulya, K., 2017. A novel pleiotropic effect of aspirin: Beneficial regulation of pro- and anti-inflammatory mechanisms in microglial cells. Brain Res. Bull. 132, 61–74. https://doi.org/10.1016/j.brainresbull.2017.05.009. Epub 2017 May 18 PMID: 28528204.
Kovács-Sólyom, F., Blaskó, A., Fajka-Boja, R., Katona, R.L., Végh, L., Novák, J., Szebeni, G.J., Krenács, L., Uher, F., Tubak, V., Kiss, R., Monostori, E., 2010. Mechanism of tumor cell-induced T-cell apoptosis mediated by galectin-1. Immunol. Lett. 127 (2), 108–118. https://doi.org/10.1016/j.imlet.2009.10.003. Epub 2009 Oct 27 PMID: 19874850.
Kreutzberg, G.W., 1996. Microglia: a sensor for pathological events in the CNS. Trends Neurosci. 19 (8), 312–318. https://doi.org/10.1016/0166-2236(96)10049-7. PMID: 8843599.
Leng, F., Edison, P., 2021. Neuroinflammation and microglial activation in Alzheimer disease: where do we go from here? Nat. Rev. Neurol. 17 (3), 157–172. https://doi.org/10.1038/s41582-020-00435-y. Epub 2020 Dec 14 PMID: 33318676.
Li, Y., Chen, N., Wu, C., Lu, Y., Gao, G., Duan, C., Yang, H., Lu, L., 2020. Galectin-1 attenuates neurodegeneration in Parkinsons disease model by modulating microglial MAPK/IκB/NFκB axis through its carbohydrate-recognition domain. Brain Behav. Immun. 83, 214–225. https://doi.org/10.1016/j.bbi.2019.10.015. Epub 2019 Oct 25 PMID: 31669519.
Linnartz, B., Neumann, H., 2013. Microglial activatory (immunoreceptor tyrosine-based activation motif)- and inhibitory (immunoreceptor tyrosine-based inhibition motif)-signaling receptors for recognition of the neuronal glycocalyx. Glia 61 (1), 37–46. https://doi.org/10.1002/glia.22359. Epub 2012 May 21 PMID: 22615186.
Linnartz, B., Bodea, L.G., Neumann, H., 2012. Microglial carbohydrate-binding receptors for neural repair. Cell Tissue Res. 349 (1), 215–227. https://doi.org/10.1007/s00441-012-1342-7. Epub 2012 Feb 14 PMID: 22331363.
Liu, F.T., Patterson, R.J., Wang, J.L., 2002. Intracellular functions of galectins. BBA 1572 (2–3), 263–273. https://doi.org/10.1016/s0304-4165(02)00313-6. PMID: 12223274.
López-Otín, C., Blasco, M.A., Partridge, L., Serrano, M., Kroemer, G., 2013. The hallmarks of aging. Cell 153 (6), 1194–1217. https://doi.org/10.1016/j.cell.2013.05.039. PMID: 23746838; PMCID: PMC3836174.
Lowry, O.H., Rosebrough, N.J., Farr, A.L., Randall, R.J., 1951. Protein measurement with the Folin phenol reagent. J. Biol. Chem. 193 (1), 265–275. PMID: 14907713.
Lublin, F.D., Reingold, S.C., Cohen, J.A., Cutter, G.R., Sorensen, P.S., Thompson, A.J., Wolinsky, J.S., Balcer, L.J., Banwell, B., Barkhof, F., Bebo, B., Calabresi, P.A., Clanet, M., Comi, G., Fox, R.J., Freedman, M.S., Goodman, A.D., Inglese, M., Kappos, L., Kieseier, B.C., Lincoln, J.A., Lubetzki, C., Miller, A.E., Montalban, X., O'Connor, P.W., Petkau, J., Pozzilli, C., Rudick, R.A., Sormani, M.P., Stuve, O., Waubant, E., Polman, C.H., 2014. Defining the clinical course of multiple sclerosis: The 2013 revisions. Neurology 83 (3), 278–286.
McGraw, J., Oschipok, L.W., Liu, J., Hiebert, G.W., Mak, C.F., Horie, H., Kadoya, T., Steeves, J.D., Ramer, M.S., Tetzlaff, W., 2004. Galectin-1 expression correlates with the regenerative potential of rubrospinal and spinal motoneurons. Neuroscience 128 (4), 713–719. https://doi.org/10.1016/j.neuroscience.2004.06.075. PMID: 15464279.
Minciullo, P.L., Catalano, A., Mandraffino, G., Casciaro, M., Crucitti, A., Maltese, G., Morabito, N., Lasco, A., Gangemi, S., Basile, G., 2016. Inflammaging and Anti-Inflammaging: The Role of Cytokines in Extreme Longevity. Arch. Immunol. Ther. Exp. (Warsz) 64 (2), 111–126. https://doi.org/10.1007/s00005-015-0377-3. Epub 2015 Dec 12 PMID: 26658771.
Ownby, R.L., 2010. Neuroinflammation and cognitive aging. Curr. Psychiatry Rep. 12 (1), 39–45. https://doi.org/10.1007/s11920-009-0082-1. PMID: 20425309.
Park, J.W., Voss, P.G., Grabski, S., Wang, J.L., Patterson, R.J., 2001. Association of galectin-1 and galectin-3 with Gemin4 in complexes containing the SMN protein. Nucleic Acids Res. 29 (17), 3595–3602. https://doi.org/10.1093/nar/29.17.3595. PMID: 11522829; PMCID: PMC55878.
Perillo, N.L., Pace, K.E., Seilhamer, J.J., Baum, L.G., 1995. Apoptosis of T cells mediated by galectin-1. Nature 378 (6558), 736–739. https://doi.org/10.1038/378736a0. PMID: 7501023.
Prinz, M., Priller, J., Sisodia, S.S., Ransohoff, R.M., 2011. Heterogeneity of CNS myeloid cells and their roles in neurodegeneration. Nat. Neurosci. 14 (10), 1227–1235. https://doi.org/10.1038/nn.2923. PMID: 21952260.
Rabinovich, G., Castagna, L., Landa, C., Riera, C.M., Sotomayor, C., 1996. Regulated expression of a 16-kd galectin-like protein in activated rat macrophages. J. Leukoc. Biol. 59 (3), 363–370.
Rabinovich, G.A., Ramhorst, R.E., Rubinstein, N., Corigliano, A., Daroqui, M.C., Kier-Joffé, E.B., Fainboim, L., 2002. Induction of allogenic T-cell hyporesponsiveness by galectin-1-mediated apoptotic and non-apoptotic mechanisms. Cell Death Differ. 9 (6), 661–670. https://doi.org/10.1038/sj.cdd.4401009. PMID: 12032675.
R.M. Ritzel S.J. Doran E.P. Glaser V.E. Meadows A.I. Faden B.A. Stoica D.J. Loane Old age increases microglial senescence, exacerbates secondary neuroinflammation, and worsens neurological outcomes after acute traumatic brain injury in mice Neurobiol Aging. 77 2019 194 –206 10.1016/j.neurobiolaging.2019.02.010 Epub 2019 Feb 20. PMID: 30904769; PMCID: PMC6486858.
Sakaguchi, M., Shingo, T., Shimazaki, T., Okano, H.J., Shiwa, M., Ishibashi, S., Oguro, H., Ninomiya, M., Kadoya, T., Horie, H., Shibuya, A., Mizusawa, H., Poirier, F., Nakauchi, H., Sawamoto, K., Okano, H., 2006. A carbohydrate-binding protein, Galectin-1, promotes proliferation of adult neural stem cells. PNAS 103 (18), 7112–7117. https://doi.org/10.1073/pnas.0508793103. Epub 2006 Apr 24. PMID: 16636291; PMCID: PMC1447526.
Schnaar, R.L., 2004. Glycolipid-mediated cell-cell recognition in inflammation and nerve regeneration. Arch. Biochem. Biophys. 426 (2), 163–172. https://doi.org/10.1016/j.abb.2004.02.019. PMID: 15158667.
Smith, A.M., Dragunow, M., 2014. The human side of microglia. Trends Neurosci. 37 (3), 125–135. https://doi.org/10.1016/j.tins.2013.12.001. Epub 2014 Jan 2 PMID: 24388427.
Starossom, S.C., Mascanfroni, I.D., Imitola, J., Cao, L., Raddassi, K., Hernandez, S.F., Bassil, R., Croci, D.O., Cerliani, J.P., Delacour, D., Wang, Y., Elyaman, W., Khoury, S.J., Rabinovich, G.A., 2012. Galectin-1 deactivates classically activated microglia and protects from inflammation-induced neurodegeneration. Immunity 37 (2), 249–263. https://doi.org/10.1016/j.immuni.2012.05.023. Epub 2012 Aug 9. PMID: 22884314; PMCID: PMC3428471.
Streit, W.J., Xue, Q.S., 2013. Microglial senescence. CNS Neurol. Disord. Drug Targets 12 (6), 763–767. https://doi.org/10.2174/18715273113126660176. PMID: 24047521.
Stuart, T., Butler, A., Hoffman, P., Hafemeister, C., Papalexi, E., Mauck 3rd, W.M., Hao, Y., Stoeckius, M., Smibert, P., Satija, R., 2019. Comprehensive Integration of Single-Cell Data. Cell 177 (7), 1888–1902.e21. https://doi.org/10.1016/j.cell.2019.05.031. Epub 2019 Jun 6. PMID: 31178118; PMCID: PMC6687398.
Szabo, M., Gulya, K., 2013. Development of the microglial phenotype in culture. Neuroscience 25 (241), 280–295. https://doi.org/10.1016/j.neuroscience.2013.03.033. Epub 2013 Mar 25 PMID: 23535251.
G.J. Szebeni É. Kriston-Pál P. Blazsó R.L. Katona J. Novák E. Szabó Á. Czibula R. Fajka-Boja B. Hegyi F. Uher L. Krenács G. Joó É. Monostori V.V. Kalinichenko Identification of Galectin-1 as a Critical Factor in Function of Mouse Mesenchymal Stromal Cell-Mediated Tumor Promotion PLoS ONE 7 7 e41372.
Town, T., Nikolic, V., Tan, J., 2005. The microglial "activation" continuum: from innate to adaptive responses. J. Neuroinflammation 31 (2), 24. https://doi.org/10.1186/1742-2094-2-24. PMID: 16259628; PMCID: PMC1298325.
Vas, V., Fajka-Boja, R., Ion, G., Dudics, V., Monostori, E., Uher, F., 2005. Biphasic effect of recombinant galectin-1 on the growth and death of early hematopoietic cells. Stem Cells 23 (2), 279–287. https://doi.org/10.1634/stemcells.2004-0084. PMID: 15671150.
Williamson, L.L., Sholar, P.W., Mistry, R.S., Smith, S.H., Bilbo, S.D., 2011. Microglia and memory: modulation by early-life infection. J. Neurosci. 31 (43), 15511–15521. https://doi.org/10.1523/JNEUROSCI.3688-11.2011. PMID: 22031897; PMCID: PMC3224817.
Ximerakis, M., Lipnick, S.L., Innes, B.T., Simmons, S.K., Adiconis, X., Dionne, D., Mayweather, B.A., Nguyen, L., Niziolek, Z., Ozek, C., Butty, V.L., Isserlin, R., Buchanan, S.M., Levine, S.S., Regev, A., Bader, G.D., Levin, J.Z., Rubin, L.L., 2019. Single-cell transcriptomic profiling of the aging mouse brain. Nat. Neurosci. 22 (10), 1696–1708. https://doi.org/10.1038/s41593-019-0491-3. Epub 2019 Sep 24 PMID: 31551601.
Zhou, F., Ciric, B., Zhang, G.X., Rostami, A., 2014. Immunotherapy using lipopolysaccharide-stimulated bone marrow-derived dendritic cells to treat experimental autoimmune encephalomyelitis. Clin. Exp. Immunol. 178 (3), 447–458. https://doi.org/10.1111/cei.12440. PMID: 25138204; PMCID: PMC4238872.
Zuñiga, E., Rabinovich, G.A., Iglesias, M.M., Gruppi, A., 2001. Regulated expression of galectin-1 during B-cell activation and implications for T-cell apoptosis. J. Leukoc. Biol. 70 (1), 73–79.